JOURNAL OF MATERIALS SCIENCE **26** (1991) 3253–3256

Crystalline order in rubber-modified thermoplastics

W. WENIG, H.-W. FIEDEL
Universität-GH-Duisburg, Laboratorium für Angewandte Physik, 4100 Duisburg 1, FRG

The crystalline order in blends of thermoplastics such as polyethylene (PE) and isotactic polypropylene (iPP) with trans octenylene rubber (TOR) has been investigated by small-angle X-ray scattering. Interface distribution functions have been used to evaluate the SAXS. It was found, that the crystal morphology depends strongly on sample composition. At 10% TOR content both thermoplastics change their supermolecular structure in a characteristic way: while in the PE/TOR blends the crystal morphology of polyethylene becomes bimodal, the lamellar order is increased in the iPP/TOR blends. This behaviour is a consequence of finer dispersion of TOR in the matrix which causes the interface area to increase.

1. Introduction

It is well known that rubber modification of such thermoplastics as linear polyethylene (PE) and isotactic polypropylene (iPP) leads to an improvement of the impact strength, while other mechanical parameters such as the elastic modulus are increasingly lowered proportional to the rubber concentration in the compound [1–7]. Martuscelli *et al.* [8] found for blends of iPP with ethylene propylene diene terpolymer (EPDM) and polyisobutylene (PIB) drastic modifications of the morphology, nucleation density, spherulitic growth rate and thermal behaviour of iPP.

For blends of iPP with trans octenylene rubber (TOR) we found [9], that mechanical parameters such as the elastic modulus, E, are strongly dependent on the composition of the samples. Instead of a monotonically decreasing curve, E surpasses a maximum at 10% TOR concentration. It is expected that this behaviour is correlated to the crystalline order in the blends. In this paper, we present results of morphological investigations of polyethylene and polypropylene modified with trans octenylene rubber. The crystal superstructure has been measured by small-angle X-ray scattering. The new method of interface distribution functions [10–14] has been employed to evaluate the SAXS of the blends.

2. Experimental procedure

2.1. Sample preparation

Linear polyethylene with a molecular weight $\bar{M}_w = 127\,000$ and isotactic polypropylene with $\bar{M}_w = 468\,000$ were dissolved in hot xylene together with appropriate weight fractions of TOR ($\bar{M}_w = 89\,000$, trans-content 80%) and precipitated into a large excess of methanol. A quantity of the dried material was placed between the plates of a hydraulic press and heated to a temperature well above the melting point of polyethylene and polypropylene, respectively, at a pressure of 10 kN. After switching off the press, the sample was allowed to cool down to room temperature. The thicknesses of the samples amounted to 1 mm.

2.2. Measurements

The small-angle X-ray scattering was measured by use of a Kratky camera. The setting of the camera was such, that sufficient high resolution was ensured (entrance slit width 30 µm, detector slit width 75 µm, distance of sample to detector 22 mm).

The measurements were controlled by a computer and the cooling water temperature was kept constant through a constant-temperature unit. CuK_α radiation was used and monochromatization achieved by using an Ni-filter in conjunction with pulse height analysis.

Each curve was recorded several times in an angular range $7 \times 10^3\ \mathrm{nm}^{-1} \leqslant s \leqslant 400 \times 10^{-3}\ \mathrm{nm}^{-1}$ ($s = 2 \sin \theta/\lambda$, 2θ being the scattering angle and λ the X-ray wavelength).

3. Results and discussion

The interface distribution function (IDF) [10–14] is a useful tool to evaluate the small-angle X-ray scattering of polymer blends with two or more crystallizable components [14]. It is defined as

$$g_1(r) = \int_0^\infty G_1(s) \cos(2\pi rs) \mathrm{d}s \qquad (1)$$

where $G_1(s)$ is the interference function. Equation 1 holds for unsmeared scattering curves; for measurements with slit-collimated cameras Equation 1 represents a good approximation [14].

$G_1(s)$ is determined as follows

$$G_1(s) = \frac{16\pi^2 t}{V}[C - D \exp(-As^2) - Is^n] \qquad (2)$$

V is the scattering volume, t the average "stack height"

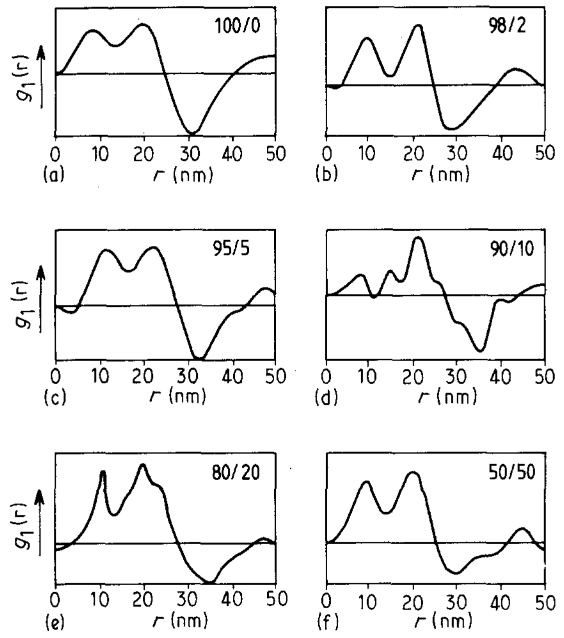

Figure 1 Interface distribution functions of PE/TOR blends.

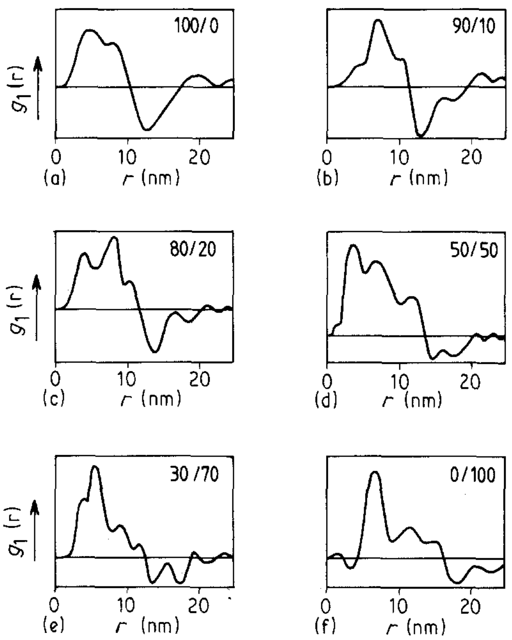

Figure 2 Interface distribution functions of iPP/TOR blends.

of lamellar stacks, I the background-corrected intensity. For slit-smeared intensities, $n = 3$.

To determine $G_1(s)$ from the measured intensity, we use a function, $I_{\mathrm{Bas}}(s)$, which is proportional to the gas scattering of the identical sample volume, containing statistically distributed scatterers

$$I_{\mathrm{Bas}}s^3 = C - (C - E)\exp(-As^2) \qquad (3)$$

with $D = C - E$. E is connected with the average chord length

$$E = \frac{k}{4\pi^2 l_{\mathrm{P}}} \qquad (4)$$

where k is Porod's constant and l_{P} is the average chord length.

The constant A is obtained from

$$A = \frac{1}{2}\left(\frac{\pi}{4}\,\frac{C - E}{Cs_{\max} - \int_0^{s_{\max}} Is^3 \mathrm{d}s}\right)^2 \qquad (5)$$

The interface distribution function is then calculated using Equation 1.

We first discuss the system PE/TOR. In Fig. 1 the interface distribution functions are displayed. Fig. 1a shows the IDF for polyethylene. Two maxima and one minimum is seen, which yield the superstructural distances in the sample. Taking into account the high crystallinity of PE, the position of the first maximum denotes the average distance of the crystals, d_{a}, while the second maximum yields the mean lamellar thickness, d_{c} [15]. The long period, L, is obtained from the position of the minimum, it should be the sum of the two values derived from the maxima. We thus find for $d_{\mathrm{a}} = 9.5$ nm, for $d_{\mathrm{c}} = 20.8$ nm, and for $L = 31.5$ nm (cf. Table I). These values are typical for PE and indicate a well-ordered morphology throughout the sample. The IDF spectrum of TOR with crystal thickness at $r = 6.2$ nm, amorphous distance at $r = 12.1$ nm and the long period at $r = 18.3$ nm (cf. Fig. 2f) cannot be separated from any of the PE/TOR curves. This might be due to the positions of the peaks, which partly coincide with PE maxima or minima, although TOR is crystallizable to an extent of 30% [16]. The PE superstructure seems not to be influenced by the TOR component except for TOR contents of 10% and, less pronounced, 20%. At these compositions additional maxima and minima occur in the IDF which, however, cannot be attributed to the TOR component. Obviously, the PE morphology in these samples becomes bimodal or even multimodal. Additional measurements on separately prepared samples have shown that these additional maxima may occur at various distances and that only those peaks are invariant towards sample preparation, which can be resolved in the interface distribution functions of other compositions. This is an indication that specific interactions between PE and TOR occur only at 10% TOR content in the blend. A similar effect has been found by Martuscelli *et al.* [8] for rubber-modified polypropylene and has been discussed to be a consequence of partial miscibility of both components. Crystallization kinetical experiments have shown, that the nucleation density is increased at 10% TOR content due to surface nucleation at the interfaces of both components [17]. Also a diffusion of TOR molecules into PE at these interfaces is possible, which could very well lead to the formation of an additional morphology.

TABLE I PE/TOR: results of interface distribution function calculations

c_{TOR}	d_{c} (nm)	d_{a} (nm)	L (nm)
0	20.8	9.5	31.5
0.02	20.5	9.5	30.0
0.05	22.2	11.0	32.5
0.1	21.4	13.8	35.0
0.2	21.2	10.6	34.0
0.5	21.0	10.0	31.4

TABLE II iPP/TOR: results of interface distribution function calculations

c_{TOR}	d_c (nm) iPP	d_c (nm) TOR	d_a (nm) iPP	d_a (nm) TOR	L (nm) iPP	L (nm) TOR
0	8.0	–	4.8	–	12.8	–
0.025	7.8	8.0	4.6	9.5	12.6	17.5
0.075	8.2	7.6	4.1	10.6	12.1	18.2
0.1	9.1	6.8	4.6	10.0	12.8	16.8
0.15	8.0	6.9	4.2	11.0	12.2	17.9
0.2	7.9	8.0	4.4	10.5	12.6	18.5
0.3	8.3	7.2	4.5	11.4	13.0	18.4
0.4	8.3	6.2	4.2	11.5	12.5	18.0
0.5	8.7	6.2	3.8	11.8	12.4	17.6
0.7	9.1	5.3	4.1	11.7	13.2	17.0
1.0	–	6.2	–	12.1	–	18.3

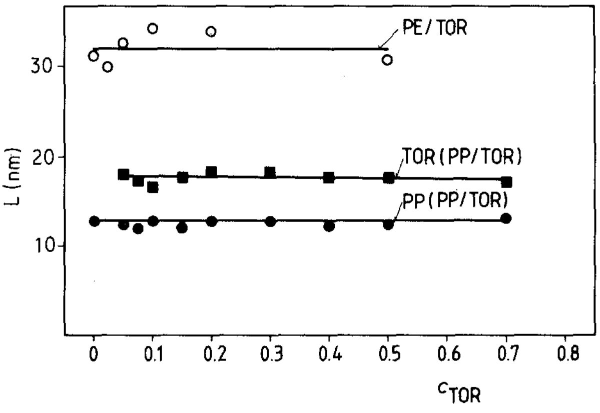

Figure 5 Long-period as a function of TOR concentration.

We therefore assume that this effect is a consequence of a composition dependent dispersion of TOR in PE rather than a semicompatibility of both components.

A different pattern is obtained for the PP/TOR blends (Fig. 2). Here, the interface distribution functions of PP (Fig. 2a) and TOR (Fig. 2f) can be well separated in the blends down to 2.5% TOR content (cf. Table II). It is therefore possible to derive the parameters d_c, d_a and L separately for iPP and TOR. These values are displayed in Figs 3–5 together with those obtained for PE (cf. Table II for a listing of the values). We see, that for PE/TOR as well as for iPP/TOR, all parameters vary only slightly with the composition. This confirms our assumption that the components in both systems are incompatible.

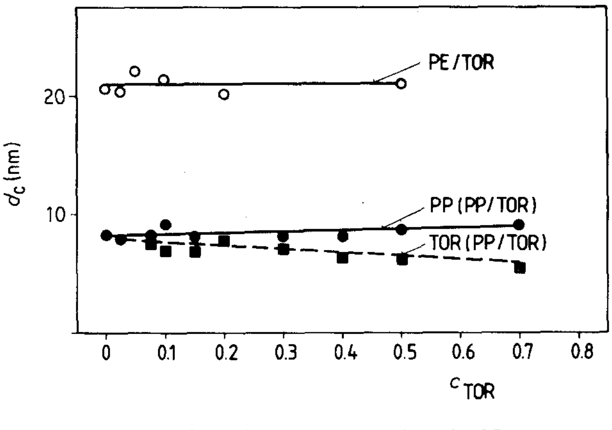

Figure 3 Mean lamellar thickness as a function of TOR concentration.

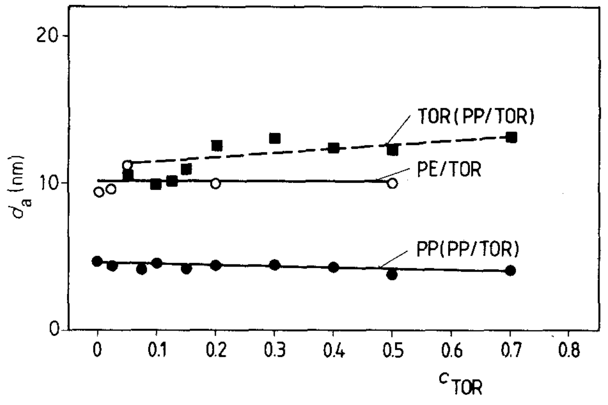

Figure 4 Mean interlamellar distance as a function of TOR concentration.

It is possible to obtain information about the mutual arrangement of the lamellar crystals by calculating the "stack height" [9, 14] from the peak heights of the interface distribution function. This parameter describes the crystalline order in a lamellar domain and is proportional to the number of lamellar crystals arranged in a parallel manner.

The stack height, t, can be derived from the exponential decrease of the peak heights w_i of the interface distribution function [14]. For non-normalized interface distribution functions, t is obtained from the comparison of peaks with heights w_1 and w_2 having equal signs

$$w_1 = w_0 \exp\left(-r_1/t\right) \tag{6}$$

$$w_2 = w_0 \exp\left(-r_2/t\right) \tag{7}$$

$$\frac{w_1}{w_2} = \exp\left(\frac{r_2 - r_1}{t}\right) \tag{8}$$

where w_0 is the height of the exponentially decreasing function at $r = 0$. From Equation 8 we get

$$\ln\frac{w_1}{w_2} = \frac{r_2 - r_1}{t} \tag{9}$$

$$t = (r_2 - r_1)/\ln\frac{w_1}{w_2} \tag{10}$$

The results of these calculations are displayed in Fig. 6. For PE/TOR, t is constant as a function of

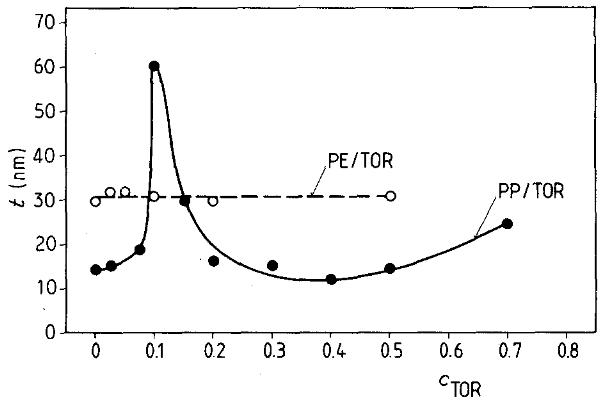

Figure 6 Stack height as a function of TOR concentration.

sample composition, but for iPP/TOR, t surpasses a maximum at $c_{TOR} = 0.1$. The number of orientation correlated crystals, which is calculated by $Z = t/L$, increases at this TOR concentration on from $Z = 1.25$ for iPP to $Z \sim 5$ for the sample containing 10% TOR. Because this behaviour cannot be attributed to any compatibility of both components, an explanation can only be found in a change of the agglomeration of the TOR in iPP, which means that the dispersion of TOR in iPP is dependent on sample composition. It is interesting that this occurs at the concentration of the phase inversion: considering the molecular weights, and taking into account the densities of iPP ($\rho_{iPP} = 0.905\ \mathrm{g\,cm^{-3}}$) and TOR ($\rho_{TOR} = 0.91\ \mathrm{g\,cm^{-3}}$), one finds equal numbers of molecules at a TOR concentration of 16.1%. Because the molecular weight distribution of TOR is bimodal [16], this value shifts towards $c_{TOR} = 0.1$. As a consequence, the interface area between the components is enhanced, affecting the crystallization kinetics of the polypropylene which in turn influences the crystal morphology of the superstructure.

4. Conclusions

1. The crystalline order of polyethylene and polypropylene blended with TOR is influenced by the rubber component.

2. At 10% TOR, polyethylene exhibits a bimodal crystal morphology. The reason for this additional structure may be the diffusion of TOR molecules into polyethylene.

3. For iPP/TOR blends the stack height of the crystal lamellae increases strongly at 10% TOR content indicating a better orientation correlation of the crystals.

4. The reason for these effects is the concentration dependent dispersion of TOR in PE and iPP. At 10% TOR content the rubber is more finely dispersed in the sample than for other compositions enhancing the interface area.

5. We found no indication for the compatibility of TOR with PE or iPP, as has been found by Martuscelli for other rubbers.

References

1. C. B. BUCKNALL, "Toughened Plastics" (Applied Science, London, 1977).
2. B. PUKANSKY, *Polym. Compos.* **7** (1986) 106.
3. P. GALLI, S. DANESI and T. SIMONAZZI, *Polym. Engng Sci.* **24** (1984) 544.
4. R. KOSFELD, K. SCHAEFER, E. A. HEMMER and M. HESS, in "Integration of Fundamental Polymer Science and Technology" edited by Kleintjens, Lemstra, Rolduc Polymer Meeting 4 (Elsevier, 1989).
5. J. E. STAMHUIS, *Polym. Compos.* **5** (1984) 202.
6. *Idem., ibid.* **9** (1988) 72.
7. *Idem., ibid.* **9** (1988) 280.
8. E. MARTUSCELLI, C. SILVESTRE and L. BIANCHI, *Polymer* **24** (1983) 1458.
9. H.-W. FIEDEL, Thesis, University of Duisburg (1988).
10. W. RULAND, *Colloid Polym. Sci.* **255** (1977) 417.
11. *Idem., ibid.* **256** (1978) 932.
12. M. STRIBECK and W. RULAND, *J. Appl. Crystallogr.* **11** (1978) 535.
13. *Idem.*, Thesis, University of Marburg (1980).
14. H.-W. FIEDEL and W. WENIG, *Colloid Polym. Sci.* **267** (1989) 389.
15. W. WENIG and T. SCHÖLLER, *Angew. Makromol. Chem.* **130** (1985) 155.
16. W. WENIG, H.-W. FIEDEL and J. PETERMANN, *Colloid Poly. Sci.* **266** (1988) 227.
17. W. WENIG and H.-W. FIEDEL, *Makromol. Chem.*

Received 20 March
and accepted 9 April 1990